

Forced Air Cooling of CPUs With Heat Sinks: A Numerical Study

Emre Ozturk and Ilker Tari

Abstract—A common ATX form factor personal computer system is modeled in detail. The flow and temperature fields inside the chassis are numerically investigated as a conjugate heat transfer problem. The computational effort is concentrated on the forced air cooling of the CPU using a heat sink. Three different commercial heat sink designs are analyzed by using commercial computational fluid dynamics software packages Icepak and Fluent. The grid independent, well converged, and well posed simulations are performed, and the results are compared with the experimental data. It is observed that flow obstructions in the chassis and the resulting air recirculation affect the heat sink temperature distribution. The specific thermal resistance values for the heat sinks are compared. It is observed that although they have different geometries, all of the three heat sinks have similar specific thermal resistances. The best heat sink is selected and modified in order to have a lower maximum temperature distribution in the heat sink by changing the geometry and the material. Especially, replacing aluminum with copper as the heat sink material improved the performance. The importance of modeling the entire chassis is demonstrated by comparing the simulation results with the results from a model of only the CPU-heat-sink-fan assembly.

Index Terms—Central processing unit (CPU) cooling, computational fluid dynamics, conjugate heat transfer, forced convection, heat sink improvement.

NOMENCLATURE

CFD	Computational Fluid Dynamics.
CPU	Computer Processing Unit.
L	Characteristic length, m.
Gr	Grashof Number.
Nu	Nusselt Number.
Pr	Prandtl Number.
R	Ideal gas constant.
R_{th}	Specific thermal resistance, $(m^2 \cdot K)/W$.
Ra	Rayleigh Number.
Re	Reynolds Number.

Manuscript received February 3, 2007; revised April 12, 2008. Current version published September 17, 2008. Some parts of this work appeared in the Proceedings of ASME 2005 Summer Heat Transfer Conference, San Francisco, CA, July 17–22, 2005. This work was recommended for publication by Associate Editor T. Lee upon evaluation of the reviewers' comments.

E. Ozturk is with Anova CAD-CAE-TEST, ODTU-OSTIM, Ankara 06370, Turkey (e-mail: emre@anova.com.tr).

I. Tari is with the Mechanical Engineering Department, Middle East Technical University, Ankara 06531, Turkey (e-mail: itari@metu.edu.tr).

Color versions of one or more of the figures in this paper are available online at <http://ieeexplore.ieee.org>.

Digital Object Identifier 10.1109/TCAPT.2008.2001840

S	Source term.
T	Temperature, K.
\vec{v}	Velocity vector.
G	Gravitational acceleration, m/s^2 .
H	Convection heat transfer coefficient, $W/(m^2 \cdot K)$.
h_o	Total enthalpy, J/kg.
K	Thermal conductivity, $W/(m \cdot K)$.
u, v, w	Velocity components, m/s.
P	Pressure, Pa.

Greek Symbols

α	Thermal diffusivity, m^2/s .
β	Volumetric thermal expansion coefficient, K^{-1} .
ΔT	Rise above ambient temperature, K.
μ	Viscosity, $kg/(s \cdot m)$.
ν	Kinematic viscosity, m^2/s .
ρ	Density, kg/m^3 .
τ	Shear stress, N/m^2 .

I. INTRODUCTION

THE central processing units (CPUs) of computers must be cooled to satisfy the maximum operating temperature limit while removing the heat dissipated by the CPU. Among all the available cooling methods, forced convection air cooling is the most common approach. In this direct heat removal approach, a fan is installed to a heat sink forming an assembly that is attached to the CPU. Air is forced through the heat sink by the fan; thus, the heat is directly transferred to the final heat transfer medium, air.

Until recently, heat dissipation values of CPUs were increasing together with their computational powers. Considering that trend, Webb [1], for future CPUs, proposed the indirect heat removal instead of the direct heat removal provided by heat sink-fan assemblies that may not be adequate to remove high heat fluxes. Gurrum *et al.* [2] projected that heat dissipation rates for computer CPUs may be as high as 180 W for the near future and as high as 288 W by the year 2016. However, the recent advances in CPU architectures of both of the major CPU manufacturers actually reduced the heat dissipation requirements, extending the life of active heat sink CPU cooling as a viable option for heat removal from CPUs.

Analyzing active heat sink CPU cooling to obtain the temperature distribution in the heat sink is a conjugate heat transfer

problem involving all three modes of heat transfer: conduction in the heat sink, forced convection to chassis air and radiation to the chassis walls, and the other components. Eventually, heat is transferred to the ambient air outside the chassis.

The present work aims to analyze the selected CPU heat sink designs by using commercial CFD software packages and to improve them by using the results of the analyses. There are many different commercial heat sink designs in the market. In this paper, three commercially available active heat sinks are investigated, namely Alpha PAL8952, Coolermaster DP5-6H11 and Evercool NW9F715CA. There are many parameters affecting the performance of a heat sink. The fin shape, the number of fins, the fin and base materials, and the base thickness are considered as the performance improvement paths for the selected heat sinks. To be able to simulate the conditions inside the chassis and to include the flow obstructions around the heat sink, not only the CPU-heat sink-fan assembly but the entire computer chassis is considered in modeling.

II. LITERATURE

Moffat [3] claims that the flow and heat transfer situations encountered in electronics cooling applications are much more challenging than those in heat exchangers and as complex as those encountered in gas turbine blade cooling. Since it is almost impossible to get a detailed solution of the temperature and velocity fields in a complicated electronic box, like a computer chassis, new methods for thermal design of such systems are emerging. Although known for years, computational fluid dynamic (CFD) simulations have not entered electronics cooling area for a long time. Before the last decade, it was very expensive to perform CFD calculations, but with the introduction of high power workstations and personal computers, the cost of such computations has been drastically reduced [4]. Nakayama *et al.* [5] suggested forming a data base from the results of a series of CFD analyses for different geometries and heat flow paths. The simulations can be run by a CFD specialist, and the database can be made available to the packaging designer. As a case study, they considered a portable computer and performed the simulations using Fluent.

Several researchers have worked on conjugate heat transfer in electronic systems via CFD. Among others, Yu and Webb [6] simulated a complete desktop computer system which uses an 80-W CPU. With the addition of other components (memory, chipset, AGP, PCI cards, and floppy drives) a total of 313-W heat is dissipated from the system. They solved the whole domain with a commercial software package, Icepak. To decrease the complexity of their model, they modeled CPU heat sink as a volume resistance having the same impedance with the detailed geometry.

Biswas *et al.* [7] also used Icepak to study the airflow in a compact electronic enclosure. Their aim was to investigate the pressure loss due to the presence of the inlet and the outlet grilles. They considered the use of fan curves which are obtained from the manufacturer since the fan curve may need to be modified if the fan is not closely ducted.

Argento *et al.* [8] studied system-level electronic packaging thermal design computationally and verified the model experimentally. After the verification, they worked on a redesign of an inlet plenum. Their implemented modification resulted in 56% reduction of the surface temperature.

Some studies use CFD for heat sink simulations only. Linton and Agonafer [9] compared the results of a detailed CFD modeling of a heat sink with experimental data. Then they presented a technique for representing the heat sink in a coarse manner for less time-consuming simulations. Their coarse model agrees well with the detailed model without losing the characteristics of the heat sink. Sathyamurthy and Runstadler [10] studied planar and staggered heat sink performance with Fluent. Their computational results agreed well with the experimental ones. They found that the thermal performance of staggered fin configuration is superior over planar fin configuration. However, the pressure drop requirements for the staggered fin heat sink was greater than those for the planar case. Yu *et al.* [11] combined pin fins with plane fins to obtain a heat sink design called plate-pin fin heat sink. Using experiments and CFD simulations, they showed that the plate-pin fin heat sink they proposed performs better than the plate fin heat sink they used for comparison.

Saini and Webb [12] performed a parametric study to determine heat rejection limits of air-cooled plain fin heat sinks for computer cooling. For increased base area and fan speed, they obtained 103.4 W as a limit for plane fin heat sinks and for impinging flow.

Eveloy *et al.* [13] used Flotherm software to provide a perspective on the current capabilities of CFD as a design tool to predict component temperature on printed circuit boards. Their computations predicted the component operating temperature in an accuracy range of 3 °C to 22 °C, with up to 35% error. They suggested that component junction temperature would need to be experimentally measured when used for strategic product design decisions. They think that the source of error is due to the employed turbulence models. They suggested to use flow visualization in the early design phase for identifying aerodynamically sensitive regions on the board, where temperature distributions should be handled with care.

Bar-Cohen and his coworkers [14]–[19] studied optimal numerical design of forced convection heat sinks of various plane fin or pin fin geometries. They focused on sustainability and considered energy use at all stages including manufacturing of the heat sink, to arrive “least energy optimization.”

The present study makes use of CFD for the conjugate heat transfer simulations in a whole computer chassis with the aim of obtaining the temperature distributions in the heat sinks which can be utilized to improve the existing heat sink design. Icepak is used for preprocessing, and Fluent is used for solution and postprocessing. Detailed modeling of the whole chassis together with the densely meshed CPU heat sink (about 40% of the cells are used for the heat sink) is selected over the so called zoom-in modeling that is commonly used for modeling interesting parts of the domain in detail. In the zoom-in modeling approach, first,

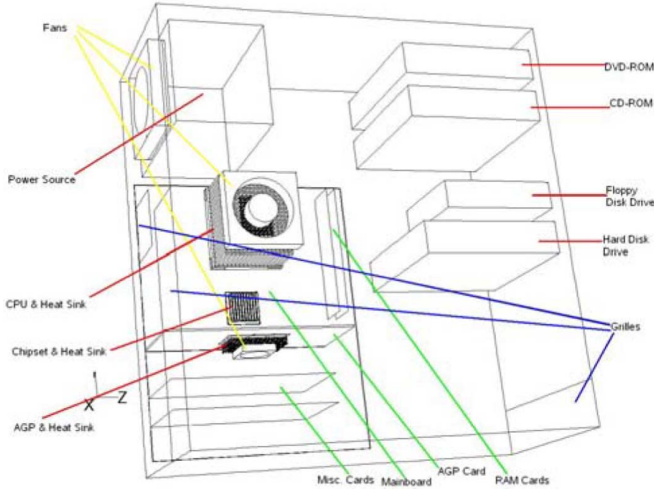


Fig. 1. Computational domain.

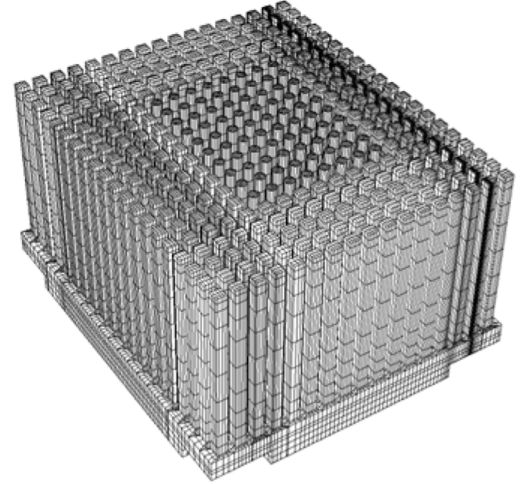


Fig. 2. Alpha PAL8952 CPU heat sink.

a simplified model of the interesting part (i.e., heat sink) is introduced into a detailed model of the domain to resolve the flow and temperature fields around the interesting part; then, the part itself is modeled in detail by using the resolved fields as the boundary conditions. In our case, to be able to start with a simplified model of the heat sink, we need to have the thermal resistance and pressure loss versus flow rate curves for the heat sinks. Since we did not perform any experiments that can provide this data, we preferred to model everything in a single simulation by increasing the mesh density around the heat sink using a non-conformal mesh.

III. CFD SIMULATION APPROACH

The CPU heat sink is attached to the CPU together with a fan. The assembly sits on the mainboard CPU socket. The mainboard and all the other components are enclosed in a chassis. Besides the CPU, there are many other heat sources. Some of them are on the mainboard (e.g., northbridge chip), some of them are attached to the mainboard (e.g., memory modules) and some of them are in the chassis volume (e.g., hard disk drive).

A. Computation Domain

The computer chassis is the computational domain. Fig. 1 shows the components of the chassis. It is a 3-D model of a common PC chassis in dimensions of $H \times W \times D = 444 \text{ mm} \times 424 \text{ mm} \times 187 \text{ mm}$. Since the aim of this study is the investigation of temperature distributions on CPU heat sinks, they are modeled in detail using their technical drawings and precise size measurements. A closer meshed view of one of the CPU heat sinks that are investigated in this study is shown in Fig. 2.

B. Governing Equations

Time-independent flow equations with turbulence are solved. The viscous dissipation term is omitted. Therefore, the governing equations for the fluid flow are the following form of the incompressible equations, respectively, continuity, x -, y -, and

z -direction momentum, and energy equations together with the equation of state:

$$\nabla \cdot (\rho \vec{V}) = 0 \quad (1)$$

$$\nabla \cdot (\rho u \vec{V}) = -\frac{\partial p}{\partial x} + \frac{\partial \tau_{xx}}{\partial x} + \frac{\partial \tau_{yx}}{\partial y} + \frac{\partial \tau_{zx}}{\partial z} + S_{Mx} \quad (2)$$

$$\nabla \cdot (\rho v \vec{V}) = -\frac{\partial p}{\partial y} + \frac{\partial \tau_{xy}}{\partial x} + \frac{\partial \tau_{yy}}{\partial y} + \frac{\partial \tau_{zy}}{\partial z} + S_{My} \quad (3)$$

$$\nabla \cdot (\rho w \vec{V}) = -\frac{\partial p}{\partial z} + \frac{\partial \tau_{xz}}{\partial x} + \frac{\partial \tau_{yz}}{\partial y} + \frac{\partial \tau_{zz}}{\partial z} + S_{Mz} \quad (4)$$

$$\nabla \cdot (\rho h_0 \vec{V}) = -p \nabla \cdot \vec{V} + \nabla \cdot (k_{\text{eff}} \nabla T) + S_h \quad (5)$$

$$p = \rho RT \quad (6)$$

where (u, v, w) are the components of the fluid velocity \vec{V} in (x, y, z) directions; ρ is the density; p is the pressure; T is the temperature, h_0 is the total enthalpy, and R is the ideal gas constant; S ; and τ are the directional body force and shear stresses. In the energy equation, (5), the effective thermal conductivity is defined as $k_{\text{eff}} = k + k_t$, where k_t is the turbulent conductivity term.

The Reynolds averaging is employed to handle the turbulence effects. In the Reynolds averaging, the solution variables are decomposed into mean and fluctuating components. For the velocity components, $u = \bar{u} + u'$ where \bar{u} and u' are the mean and fluctuating velocity components for x -direction. Likewise, for the pressure and the other scalar quantities $\phi = \bar{\phi} + \phi'$ where ϕ is a scalar such as pressure or energy.

The Reynolds Averaged Navier–Stokes (RANS) equations are solved together with the Boussinesq approximation.

C. Boundary Conditions

Since the Navier–Stokes equations are solved inside the domain, no-slip boundary condition is applied to all the walls in the domain. Therefore, at all of the surfaces, $u = v = w = 0$.

It is assumed that the system fan does not drive a flow cell around the computer chassis and the heat transfer mechanism

at the chassis outer walls is natural convection. Heat transfer coefficients at the outer walls are estimated from the empirical correlations which are available in the literature [20]. In order to use the correlations, the average wall temperature must be prescribed. To do that, a first cut analysis must be run. As the typical values of the natural convection heat transfer coefficient lie between 2 and 25 W/(m² · K), a value of 5 W/(m² · K) is selected to be the heat transfer coefficient at the computer chassis walls. The analysis by taking the ambient temperature as 30 °C gives an average temperature of 36 °C at the walls, and then heat transfer coefficients are calculated using this value and the available correlations with the uniform surface temperature assumption, and with the definitions of the Rayleigh number and the average Nusselt number as: $Ra_L = Gr_L Pr = g\beta(T_s - T_\infty)L^3/\nu\alpha$ and $\overline{Nu}_L = hL/k$, where L is the characteristic length, and h , k , g , β , ν , and α are the convection heat transfer coefficient, the fluid thermal conductivity, the gravitational acceleration, the volumetric thermal expansion coefficient, the kinematic viscosity and the thermal diffusivity, respectively. T_s and T_∞ are the surface and the ambient temperatures. Here, Ra_L is less than 10⁹; therefore, the flow is laminar. Using the correlations for laminar natural convection on the vertical plate by taking the thermal conductivity of air as $k = 0.027$ W/(m · K), the heat transfer coefficient, $h \approx 3$ W/(m² · K). The second analysis is performed by applying this value as the wall heat transfer coefficients of the computer chassis and it is seen that the average wall temperatures are very close to 36 °C; therefore, the iterations are ended.

Similarly, for the horizontal top plate the Rayleigh number is calculated as 1.5×10^5 , where the characteristic length is calculated from $L = A/P$, where A is the plate surface area, and P is the plate perimeter. The average Nusselt number is correlated to the Rayleigh number with $\overline{Nu}_L = 0.54Ra_L^{1/4}$ which gives $h = 0.05$ W/(m² · K).

The calculated heat transfer coefficients are applied to all of the exterior walls of the chassis except the bottom horizontal wall which sits on the ground that is considered to be adiabatic.

D. Interior Conditions

The heat dissipation rates and the material definitions for the objects inside the chassis are listed in Table I. A total of 252 W is dissipated.

The fans inside the domain are modeled as circular surfaces which add momentum source to the flow. The added momentum source is given as the pressure rise across the fan versus the flow rate curve. The point where the fan is going to operate is calculated iteratively from the system pressure curve. The relationship between the pressure and the flow rate is assumed to be linear. The fan conditions are given in Table II.

The condition for the power supply is handled differently. Inside of the power supply is geometrically very complicated. Therefore, it is modeled with simplifications. The power supply is a rectangular box which creates resistance to flow. The resistance is different in the y -direction. The reason for this is to allow air to pass through the power supply more easily in the

TABLE I
INTERIOR CONDITIONS

Object Name	Material	HeatDissipation Rates (W)
CPU	Silicon	70
AGP	Silicon	25
CD	Al	10
DVD	Al	10
Hard drive	Al	20
Floppy	Al	-
Chipset	Silicon	10
CPU heat sink	Al-Cu	-
AGP heat sink	Al	-
Chipset heat sink	Al	-
Power supply	Porous	75
Memory cards	FR4	6x2
Misc. cards	FR4	10x2
Mainboard	FR4	-

TABLE II
FAN CONDITIONS

Object Name	Pressure Rise (Pa)	Maximum Flow Rate (cfm)
CPU Heat sink fan	25	30
Case fan	40	40
AGP Heat sink fan	25	25

y -direction than the other directions. This is accomplished by modeling the power supply as a porous medium. The porous medium modeling adds a momentum sink to the momentum equation which creates a pressure drop proportional to the velocity. The momentum sink is composed of two parts, the first term on the right-hand side is the viscous loss term and the second term is the inertial loss term

$$S_i = - \left(\frac{\mu}{\alpha} v_i + C_2 \frac{1}{2} \rho v_{\text{mag}} v_i \right) \quad (7)$$

where α is the permeability, and v_{mag} is the velocity magnitude. When it is defined separately in different directions, anisotropic permeability is modeled. C_2 is the inertial resistance factor which is zero in our case due to the laminar flow assumption in the porous zone. In this case, the equation simplifies to the Darcy's law.

E. Discretization

Fluent uses the finite volume method, and error arises due to discretization of the governing equations. Interpolations are made to find values at the cell faces, whereas all the information is stored at the cell centers.

Interpolations have to be done for discretization. There are numerous schemes, and the easiest one is the first-order

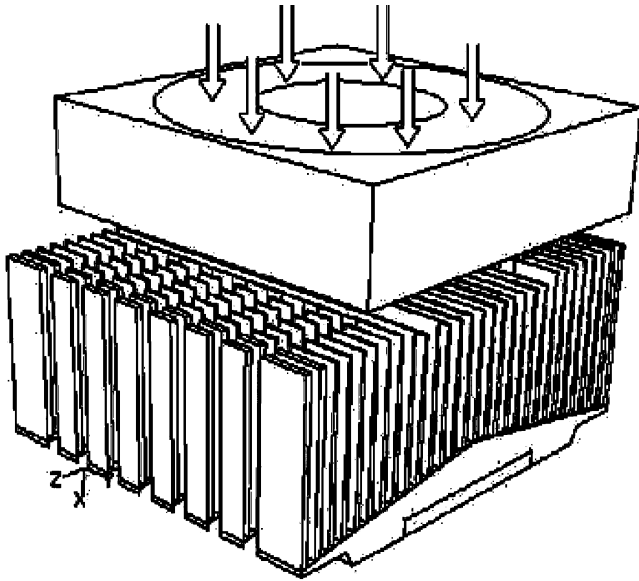


Fig. 3. Air flow direction shown on Evercool NW9F715CA heat sink fan assembly.

upwinding. The advantage of this scheme is that it converges easily. The disadvantage is that it is only first-order accurate. It is suggested to use second-order schemes for unstructured grids [21]. In our cases, the comparison of the first-order and the second-order upwinding schemes is done.

For the flow direction, shown in Fig. 3, the temperature distributions on the same heat sink, Evercool, which is solved by the first-order and the second-order upwinding schemes are compared [22]. The ranges of the local temperature values on the heat sink are similar in both cases; therefore, the first-order method is computationally less costly is used in all simulations.

F. Convergence Issues

Only a well-converged, well-posed, and grid-independent simulation can give reliable results. Convergence is determined by the order of magnitude residuals drop. Two different convergence tolerances are compared: one is 10^{-3} for flow and 10^{-6} for energy, and the other is 10^{-4} for flow and 10^{-7} for energy. Running the solver such that residuals fall one more order of magnitude means that more iterations are done to improve the solution quality. It should be noted that convergence criteria must assure that the results do not change as the iterations proceed. There is a common way of implementing this idea. Changes in some scalars such as temperature are displayed as well as the residual monitors. When the scalar values do not change as the iterations continue, then it can be stated that the solution is converged. It was seen that this trend is achieved when the continuity and momentum residuals fell below 10^{-4} and energy residual fell below 10^{-7} [22]. Therefore, all the models use the convergence criteria of 10^{-4} for the flow variables and 10^{-7} for the energy.

Authorized licensed use limited to: Morrison & Foerster LLP. Downloaded on November 17, 2025 at 16:12:00 UTC from IEEE Xplore. Restrictions apply.

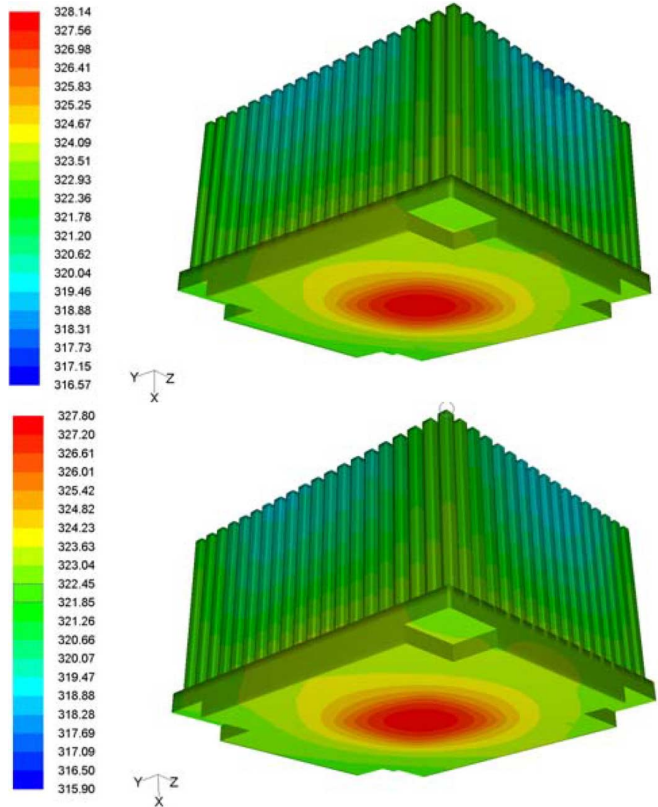


Fig. 4. Temperature distributions on Alpha PAL8952 heat sink for 900 000 cells at the top and 1.5 million cells at the bottom.

G. Grid Selection

The only way to establish grid independent solutions is to setup a model with a finer mesh and analyze it to see if there are major differences in scalar quantities and vectors. An additional test case is prepared using 1.5 million cells. The results are compared with the default 900 000 cell model. The mesh density increase mostly concentrated within the nonconformal mesh around the heat sink [22]. Fig. 4 illustrates that the temperature distributions are similar. This shows that 900 000 cells are enough for the models to be grid independent. Fig. 5 shows the temperature plots on a reference line passing through the centerline of the bottom of the heat sink (the reference line) for two different grids. The density distribution of the mesh is concentrated around the CPU heat sink, for example in the Alpha heat sink case, 340 828 out of 848 857 cells are in the nonconformal mesh of the heat sink.

H. Turbulence Modeling

The default turbulence model of all calculations is the algebraic turbulence model. It is the computationally least expensive one since no extra equations are solved in addition to continuity, momentum, and energy equations. However, in order to rely on the results that the algebraic model gives, it should be validated with higher order turbulence models. The RNG $k-\epsilon$ model is used as a test case. The temperature distributions and velocity fields are compared. The results show acceptable agreement as

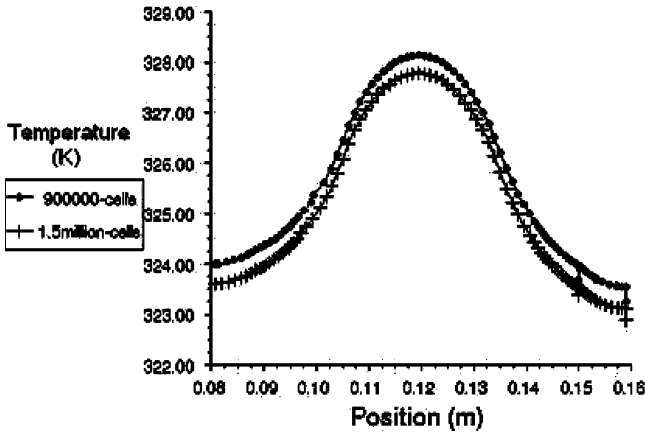


Fig. 5. Temperature plots on the reference line for two different grids.

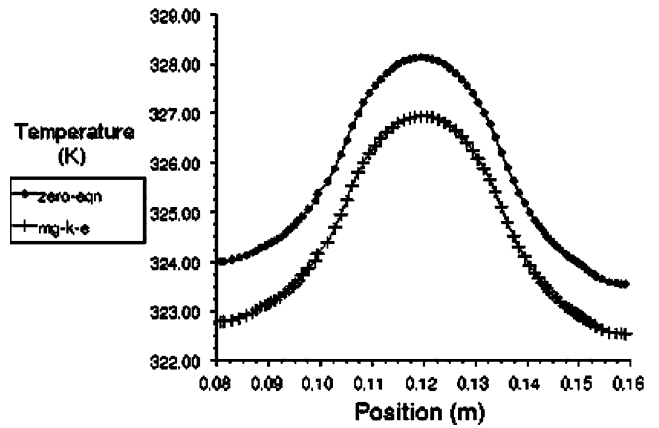


Fig. 7. Temperature plots on the reference line for the two turbulence models.

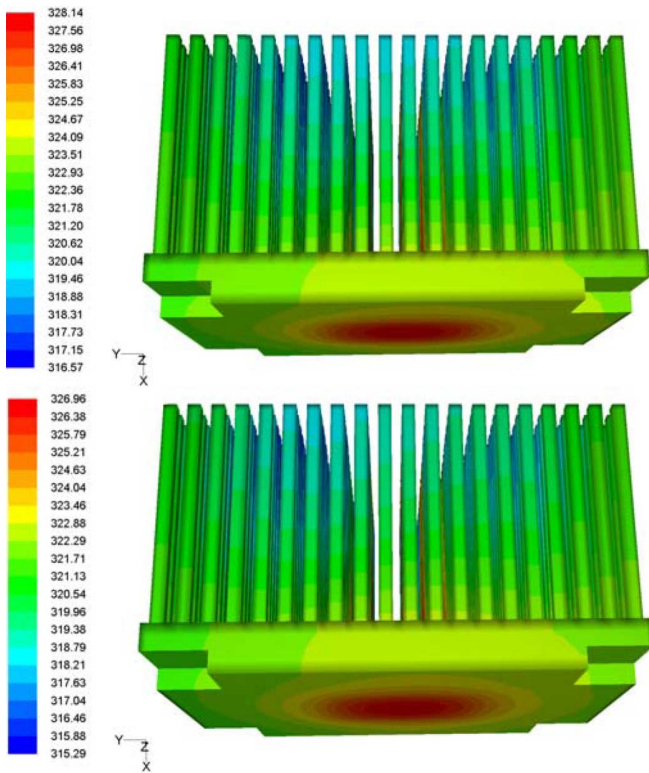


Fig. 6. Temperature distributions on Alpha PAL8952 heat sink for different Turbulence Models, ATM at the top and RNG $k-\epsilon$ at the bottom.

seen in Fig. 6. Therefore, we conclude that it is enough to use the algebraic turbulence model. Using the RNG $k-\epsilon$ model, which is a two-equation model, doubles the solution time. This corresponds to two days of continuous runs. The sole reason for that is not the extra number of equations solved, but also the slow convergence.

Fig. 7 shows the difference between the temperatures on the reference line when two different turbulence models are used.

I. Radiation Effects

Alpha heat sink is analyzed to investigate the radiation effects [22]. Radiation heat transfer helped the Alpha heat sink cool

by less than additional 0.5 K. Therefore, it is concluded that radiation could be ignored for forced cooling of CPUs.

IV. RESULTS AND DISCUSSIONS

The first group of results shown here are for temperature distributions of all of the three heat sinks for the same conditions and using the same model. That is, the results are obtained by changing the heat sink model while keeping the rest of the computational domain the same.

A. Temperature Distributions

The temperature distributions for the considered three heat sinks are shown in Fig. 8. It is obvious from Fig. 8 and Table III that Alpha heat sink outperforms the other two. The main reason for this is that it is a bigger heat sink with more heat transfer area. Evercool performed better than Coolermaster. Although the heat sink dimensions are similar for these two, Evercool has a copper-embedded base which enables higher conduction rates, and heat is conducted to the whole heat sink in a more efficient way. For all of the heat sinks, it can be stated that their centers are the hot spots since the heat source corresponds to the proximity of the base center. The fans installed on the heat sinks are identical with dimensions and fan curves. The fans have hubs where air cannot pass through and it makes the center parts hotter. In the current simulations, the swirl of the fan is not modeled since the fans are lumped parameter models. For real cases, the center would not be as hot as the present simulations predict, due to the swirl.

The asymmetric temperature distributions are due to the flow obstructions inside the computer chassis around the heat sink. The path lines of flow around Evercool together with the temperature distribution are shown in Fig. 9. In YZ view (top), the left side of the heat sink is obstructed by the computer chassis wall, whereas on the right side stands the memory cards. The power supply is located at the top. Even though it is not a solid obstruction since it is modeled as a porous medium, it blocks the flow partially. The AGP card with a relatively large heat dissipation lies below. When the computer chassis is investigated, it is observed that only the upper right part of the heat sink has

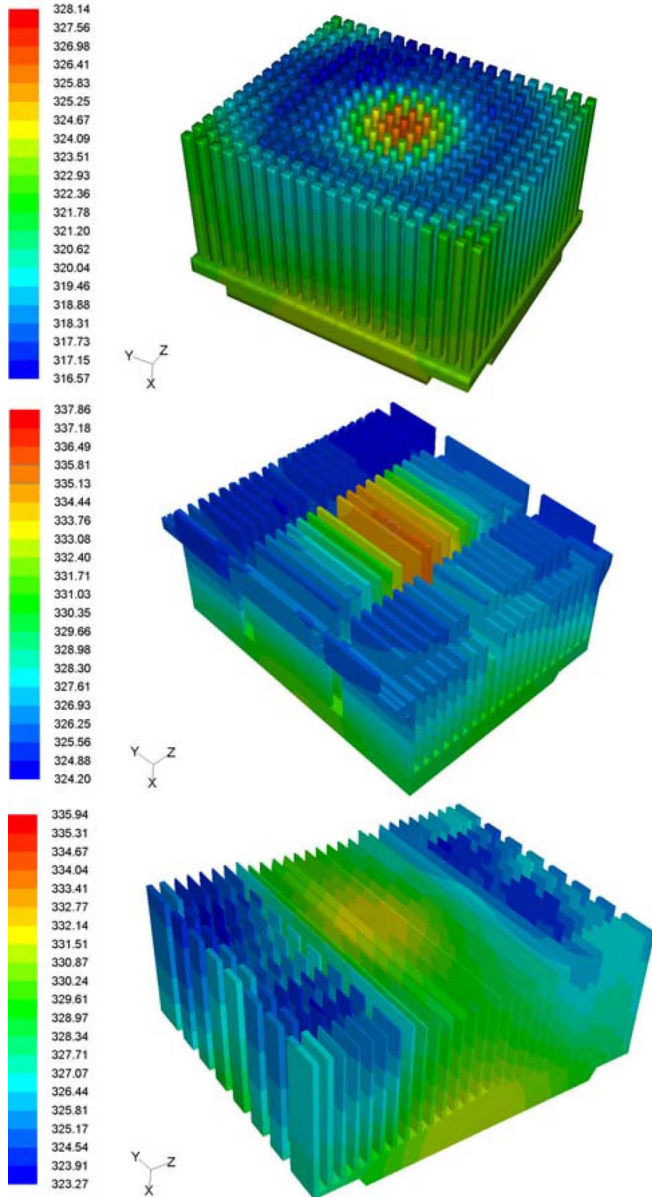


Fig. 8. Temperature distributions on different CPU heat sinks, from top to bottom, Alpha PAL8952, Coolermaster DP5-6H11 and Evercool NW9F715CA.

a free path for the air flow. Therefore, air driven by the CPU fan can travel to that side and the effect of which can also be seen in the temperature distributions of Fig. 8. On the other sides of the CPU, air returns to the proximity of the heat sink by hitting the walls or other cards; the fan sucks the returning relatively hot air and the cooling becomes less efficient at these sides of the heat sink, as can be observed in Fig. 9 XY view (bottom).

It is also observed from these results that modeling not only the CPU-heat sink assembly but the whole chassis is important for predicting heat sink performance. To investigate this issue further, in a model, everything inside the chassis is removed except the CPU, Alpha heat sink, and the fan. The mesh around this assembly is kept the same, to be able to compare the results

TABLE III
TEMPERATURE NONUNIFORMITY FOR THE THREE HEAT SINKS FOR 70-W CPU HEAT DISSIPATION

	Alpha PAL8952	Coolermaster DP5-6H11	Evercool NW9F715CA
Tmax (K)	328	338	336
Tmin (K)	316	324	323
Tmax-Tmin (K)	12	14	13
Average rise above ambient, ΔT (K)	18.7	27.2	24.6
Normalized nonuniformity (Tmax-Tmin)/ ΔT	0.64	0.51	0.53

with the detailed chassis model. This model with CPU heat dissipation values of 50 and 100 W also resembles the experimental setup that is discussed in Section V-B. The temperature distributions on the Alpha heat sink for both heat dissipation values obtained for this model are shown in Fig. 10. The chassis itself is still present with the same inlets and outlets. The air can still bounce off the chassis walls and recirculate in the chassis, but the temperature distribution is much more symmetric compared to the detailed whole chassis model. This result demonstrates that asymmetry in the whole chassis results are not only due to chassis walls but also due to the presence of all other components inside the chassis.

B. Comparison With Experimental Data

There were some experiments in the literature that have been conducted on CPU heat sinks. Among these, the data obtained by Frostytech [23] which is given in Table IV is used for comparison. Their test setup is not the whole computer chassis system, but a smaller domain, in order to simplify the experiments. They prepared a copper block to install the heat sink over, and heated the block with two different heat loads, 50 and 100 W. The rise above ambient temperature values were recorded directly. Since the test setup is an open domain, the ambient temperature is the temperature of the air blown on to the heat sink. However, in our simulations, ambient temperature is the temperature outside the domain. Hence, the air blown by the CPU fan is considerably hotter than the outside temperature which necessitates the calculation of the average temperature at the fan exit. In our simulations, the average temperature that the fan blows is calculated. This value is used as the corresponding ambient temperature of the test setup.

Although a quantitative comparison was made in Table IV, the results should be judged qualitatively while trying to select the best performer. Besides the difference in ΔT evaluations, the characteristics of the fan supplied by the heat sink manufacturer (e.g., rotation speed, flow rate, blade geometry) play an important role in the heat sink temperature distribution. Due to

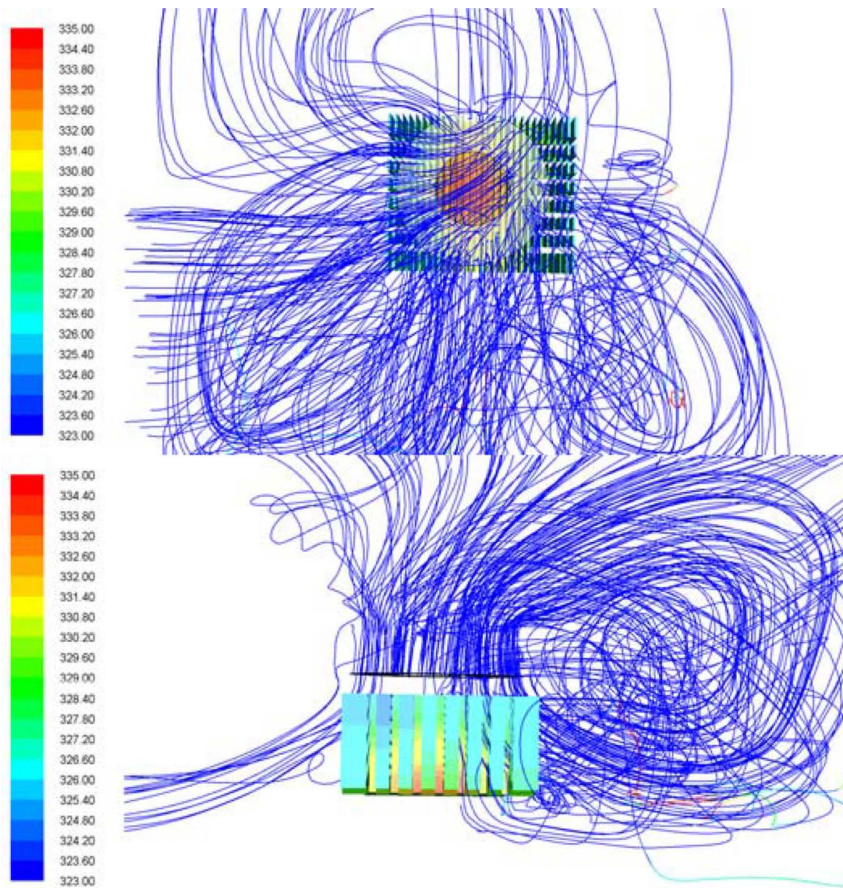


Fig. 9. Path lines and temperature distribution for Evercool NW9F715CA (YZ and XY views).

lack of information related to the fan models supplied with each heat sink, for all of the three heat sinks, identical fans are used in the numerical simulations.

When heat dissipation is increased from 50 to 100 W, it is observed that Alpha and Evercool specific thermal resistance (R_{th} in Table IV) values do not change much, indicating that their performances are not sensitive to fluctuations in the heat dissipation. Surprisingly, R_{th} of CoolerMaster reduced significantly with the heat dissipation increase. Nevertheless, it performed comparatively worse than the others at 50 W, and its sensitivity to heat dissipation changes is relatively severe that may require a transient analysis to make it acceptable for regular operation of CPUs that involves sudden changes in heat dissipation. Thus, we eliminated CoolerMaster among choices while trying to select the best performer.

Alpha and Evercool have similar specific thermal resistance results. Although the numerical results of R_{th} are in favor of Evercool, Alpha significantly outperforms the other two when ΔT values are compared. This result is not surprising because the area of Alpha is roughly 50% bigger than the other two. Since all of the three heat sinks are successful commercial products, it is also not surprising to see that their specific thermal resistances are all about $0.04 \text{ (m}^2 \cdot \text{K)/W}$, which is a good value. This shows that they all have adequate fin lengths and fin geometries, but the one with the larger area outperforms the others. Accord-

ingly, we selected Alpha as the best heat sink and tried to modify it to improve its performance further.

C. Improvement Case 1: Number of Fins

When the temperature distributions and the path lines from the fan on Figs. 8 and 9 are investigated, it is seen that densely stacked fins do not allow much air to cool the hottest center parts of the heat sink. Therefore, by removing some of the fins a gateway is opened for cooler air. 36, 52, and 56 fins are successively removed from Alpha as shown in Fig. 11.

From the temperature distributions in Table V, it is seen that removing some of the fins did not affect the overall performance of the heat sink. The total heat transfer area decreases when some fins are removed. However, due to a better flow path for the air, the performance does not change. Even though there is not a significant change in the thermal resistance, the reduction in heat sink material and weight poses an advantage for the manufacturer.

D. Improvement Case 2: Heat Sink Material

Starting with the improved design after removing 52 fins, we considered improving the thermal conductivity by using copper instead of aluminum. First, it is seen that when the four fins at the center of the heat sink are modified to be copper, the thermal performance of the heat sink is not affected, indicating that these

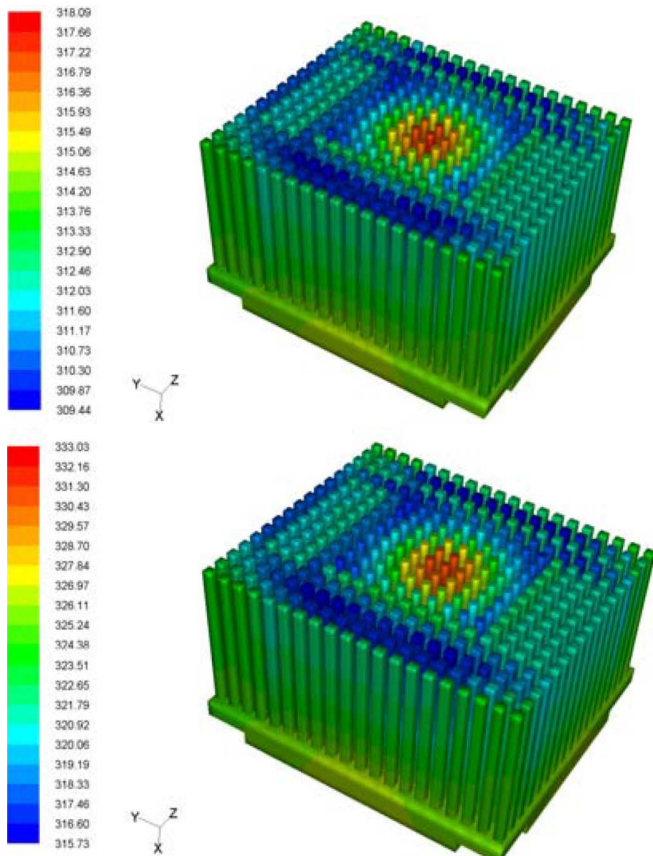


Fig. 10. Temperature distributions for the model with only the CPU, Alpha heat sink, and the fan present inside the chassis. CPU heat dissipation values are 50 W (top) and 100 W (bottom).

fins do not contribute much to the heat transfer. This result is expected from the previous analyses where removing the four center fins did not change the temperature distribution [22]. However, when all of the fins are made out of copper, the maximum temperature on the heat sink decreases by 2°C. It is also observed from Fig. 12 that the minimum temperature increases by more than 1°C. Therefore, the temperature gradients on the heat sink are observed to be smaller due to the high thermal conductivity of copper. The difference between the maximum and the minimum temperatures on the copper heat sink is less than 9 °C, whereas for the aluminum heat sink it was around 12 °C.

E. Improvement Case 3: Base Thickness

Again, by considering the case where 52 fins are removed from the aluminum Alpha heat sink, in order to investigate the base thickness effect, the base thickness of Alpha, which is normally 9 mm, is increased and decreased by 3 mm while keeping the fin lengths constant. The temperature distributions on the reference line are compared in Fig. 13. The heat sink with the thinner base has higher temperatures. The tip temperatures are also very high since there is almost no temperature gradient on the fin along the fin length. As seen from Fig. 13, the thinner base results are not acceptable, and longer fins should be used in order to decrease the maximum temperature on the heat sink together

TABLE IV
EXPERIMENTAL AND NUMERICAL RESULTS OF RISE ABOVE AMBIENT TEMPERATURE AND SPECIFIC THERMAL RESISTANCE

CPU heat dissipation	Alpha heat sink			Coolermaster DP5-6H11	Evercool NW9F715CA
	Heat sink area (m ²)	Alpha PAL8952			
50 W	ΔT Experimental (K)	12.7	23.3	19.1	
	ΔT Numerical (K)	13.1	22.8	17.4	
	ΔT Error	-3.1 %	2.1 %	8.9 %	
	R_{th} Exp. (m ² K/W)	0.0396	0.0474	0.0406	
	R_{th} Num. (m ² K/W)	0.0408	0.0463	0.0370	
100 W	ΔT Experimental (K)	25.4	34.4	38.5	
	ΔT Numerical (K)	27.2	33.9	35.3	
	ΔT Error	-7.1 %	1.5 %	8.3 %	
	R_{th} Exp. (m ² K/W)	0.0396	0.0350	0.0409	
	R_{th} Num. (m ² K/W)	0.0424	0.0344	0.0375	

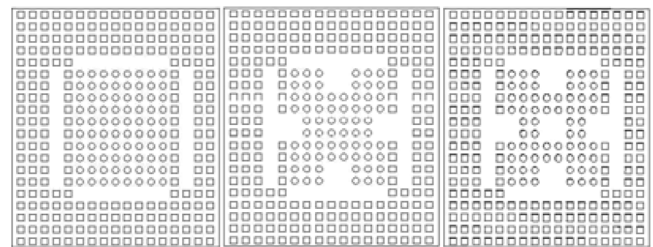


Fig. 11. Three modified versions of Alpha heat sink.

TABLE V
MAXIMUM AND MINIMUM TEMPERATURES ON MODIFIED HEAT SINKS

	36 fins less	52 fins less	56 fins less
Tmax (K)	328.71	328.94	328.93
Tmin (K)	316.03	316.04	316.02
Tmax-Tmin (K)	12.68	12.90	12.91

with a higher base thickness. For the heat sinks whose base width is larger than the footprint of the heat source, which is the

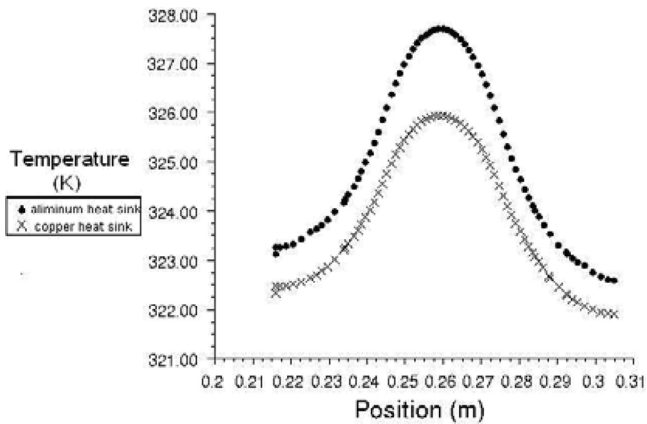


Fig. 12. Temperature plots on the reference line for heat sink material comparison.

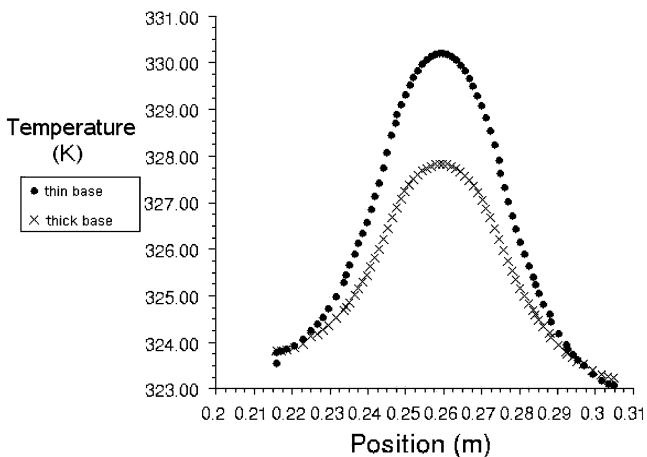


Fig. 13. Temperature plots on the base reference line for heat sinks with different base thicknesses.

case here, the in-plane conduction resistance should be considered. Therefore, higher base thicknesses decrease the in-plane resistance as observed from Fig. 13. On the other hand, if the heat source and heat sink have the same width, it is better to make the base thinner to decrease the conduction resistance from the base to the fin tip direction.

V. CONCLUSION

In this paper, CPU cooling was investigated in a complete computer chassis with three different heat sinks whose performances were compared. The influence of the mesh resolution, turbulence model choice, convergence criteria, and discretization schemes were investigated to find the best model with the least computational cost. The heat sink temperature difference results and specific thermal resistances were compared with the available experimental results. Even though the comparison was qualitative, the numerical simulation results showed agreement with the experimental data.

It was shown that the improvements on heat sink designs are possible with the help of CFD. The number of fins and their distribution, the fin material, and the base plate thickness were

investigated, and some thermal enhancements as well as weight and material savings were achieved. It is observed that successive parametric runs are necessary to be able to evaluate the effects of the design parameters on the heat sink performance. Eventually, using CFD simulations, it is possible to come up with a new heat sink design which has better thermal performance and uses less material. In the current study, it was seen that stacking too many fins is not a solution for decreasing the hot spots on the heat sink since they may prevent the passage of air coming from the fan to the hottest center parts of the heat sink. If fin material is selected to be copper rather than aluminum, then the thermal resistance of the heat sink decreases as expected. However, this makes the heat sink more expensive and heavier. The heat sink base thickness is also a parameter for improvement. When the base plate thickness was increased, the heat sink performed better. However, there are space limitations for every heat sink in a computer. Therefore, the total height of the heat sink should be considered together with the space limitations when increasing the height of the heat sink. Designing a narrower heat sink to decrease the in-plane conduction resistance is not a solution since it can accommodate fewer fins on itself which decreases the total heat transfer area. It is also observed that for all of the three heat sinks, the fin base to tip temperature difference is relatively large. Heat pipes running from the base to fin tips may be used to reduce the difference and to utilize the fin height more effectively. This is a common approach in newer heat sink designs.

System-level CFD simulations can be useful while selecting and adjusting a particular heat sink design. We observed that the velocity field around the heat sink is affected from the presence of the other components inside the chassis as well as the chassis walls which created some recirculation of hot air back into CPU heat sink. If the heat sink is plate fin type, plate fins can be oriented according to CFD results to reduce the recirculation. It is also possible to orient the fan of the heat sink to a position to increase intake of cooler air. Considering that the CPU is the largest heat source, drawing cooler ambient air directly from outside the chassis to the CPU fan with a duct is a viable option that has been recently implemented by many chassis manufacturers. With the help of CFD, these and many other types of system-level modifications can be tested by observing their overall effect on the thermal management of the chassis.

Finally, it is observed that even very complicated geometries can be modeled for the solution of conjugate heat transfer using CFD. The results are acceptable as long as attention is paid on mesh density and quality, boundary conditions, convergence quality, physical models such as turbulence, and discretization schemes. The present study together with the accompanying thesis [22] outlines the details of CFD simulation steps for a computer chassis thermal management solution by concentrating on CPU cooling. The current limitations of computer technology have prevented us from modeling the problem with fewer approximations. That is, it is not possible to solve the governing equations with direct numerical simulation or even without using any lumped parameter model. However, even

with these limitations, CFD is a useful design tool. It decreases the design time by minimizing the trial-and-error cycle, consequently reducing the cost. A prototype manufactured after every trial is the major cause of time loss that can be reduced by using CFD. One of the obstacles, refraining CFD from being used in electronic package design more readily, is the lack of error prediction. The leading CFD software vendors are trying to make error estimation possible. As demonstrated by Evely et al. [13] experimental measurements accompanying CFD analyses may make CFD a tool for every stage of the design process.

REFERENCES

- [1] R. L. Webb, "Next generation devices for electronic cooling with heat rejection to air," *Trans. ASME, J. Heat Transfer*, vol. 127, pp. 2–10, 2005.
- [2] S. P. Gurrum, S. K. Suman, Y. K. Joshi, and A. G. Fedorov, "Thermal issues in next-generation integrated circuits," *IEEE Trans. Device Mater. Rel.*, vol. 4, pp. 709–714, Dec. 2004.
- [3] R. J. Moffat, "Getting the most out of your CFD program," in *Proc. IEEE Inter Soc. Conf. Thermal Phenomena*, 2002, pp. 9–14.
- [4] M. Behnia, W. Nakayama, and J. Wang, "CFD simulations of heat transfer from a heated module in an air stream: Comparison with experiments and a parametric study," in *Proc. IEEE Inter Soc. Conf. Thermal Phenomena*, 1998, pp. 143–151.
- [5] W. Nakayama, M. Behnia, and D. Soodphakdee, "A novel approach to the design of complex heat transfer systems: portable computer design-A case study," *IEEE Trans. Compon. Packag. Technol.*, vol. 24, no. 2, pp. 199–206, Jun. 2001.
- [6] C.-W. Yu and R. L. Webb, "Thermal design of a desktop computer system using CFD analysis," in *Proc. 17th IEEE Semi-Therm Symp.*, 2001, pp. 18–26.
- [7] R. Biswas, R. B. Agarwal, A. Goswami, and V. Mansingh, "Evaluation of airflow prediction methods in compact electronic enclosures," in *Proc. 15th IEEE Semi-Therm Symp.*, 1999, pp. 48–53.
- [8] C. W. Argento, Y. K. Joshi, and M. D. Osterman, "Forced convection air-cooling of a commercial electronic chassis: An experimental and computational case study," *IEEE Trans. Compon., Packag., Manuf. Technol.-Part A*, vol. 19, no. 2, pp. 248–257, Jun. 1996.
- [9] R. L. Linton and D. Agonefer, "Coarse and detailed CFD modelling of a finned heat sink," *IEEE Trans. Compon., Packag., Manuf. Technol.-Part A*, vol. 18, no. 3, pp. 517–520, Sep. 1995.
- [10] P. Sathyamurthy, P. W. Runstadler, and S. Lee, "Numerical and experimental evaluation of planar and staggered heat sinks," in *Proc. IEEE Inter Soc. Conf. Thermal Phenomena*, 1996, pp. 132–139.
- [11] X. Yu, J. Feng, Q. Feng, and Q. Wang, "Development of a plate-pin fin heat sink and its performance comparisons with a plate fin heat sink," *Appl. Thermal Eng.*, vol. 25, pp. 173–182, 2005.
- [12] M. Saini and R. L. Webb, "Heat rejection limits of air cooled plane fin heat sinks for computer cooling," *IEEE Trans. Compon. Packag. Technol.*, vol. 26, no. 1, pp. 71–79, Mar. 2003.
- [13] V. Evely, P. Rodgers, and M. S. J. Hashmi, "Numerical prediction of electronic component heat transfer: An industry perspective," in *Proc. 19th IEEE Semi-Therm Symp.*, 2003, pp. 14–26.
- [14] A. Bar-Cohen and M. Iyengar, "Design and optimization of air-cooled heat sinks for sustainable development," *IEEE Trans. Compon. Packag. Technol.*, vol. 25, no. 4, pp. 584–591, Dec. 2002.
- [15] A. Bar-Cohen and M. Iyengar, "Least-energy optimization of air-cooled heat sinks for sustainable development," *IEEE Trans. Compon. Packag. Technol.*, vol. 26, no. 1, pp. 16–25, Mar. 2003.
- [16] M. Iyengar and A. Bar-Cohen, "Least-energy optimization of forced convection plate-fin heat sinks," *IEEE Trans. Compon. Packag. Technol.*, vol. 26, no. 1, pp. 62–70, Mar. 2003.
- [17] N. Afgan, M. G. Carvalho, S. Prstic, and A. Bar-Cohen, "Sustainability assessment of aluminum heat sink design," *Heat Transfer Eng.*, vol. 24, pp. 39–48, 2003.
- [18] W. B. Krueger and A. Bar-Cohen, "Optimal numerical design of forced convection heat sinks," *IEEE Trans. Compon. Packag. Technol.*, vol. 27, no. 2, pp. 417–425, Jun. 2004.
- [19] A. Bar-Cohen, R. Bahadur, and M. Iyengar, "Least-energy optimization of air-cooled heat sinks for sustainability-theory, geometry and material selection," *Energy*, vol. 31, pp. 579–619, 2006.
- [20] F. P. Incropera and D. P. DeWitt, *Fundamentals of Heat and Mass Transfer*, 5th ed. New York: Wiley, 2002, ch. 9.
- [21] *FLUENT 6.1 Users Guide*. Lebanon, NH: Fluent, 2004.
- [22] E. Öztürk, "CFD analyses of heat sinks for CPU cooling with Fluent," M.S. thesis, Dept. Mech. Eng., Middle East Tech. Univ, Ankara, Turkey, 2004.
- [23] Heat Sink Reviews Frostytech, 2004 [Online]. Available: www.frostytech.com



Emre Ozturk received the B.S. and M.S. degrees in mechanical engineering from the Middle East Technical University (METU), Ankara, Turkey, in 2001 and 2004. He is currently pursuing the Ph.D. degree in mechanical engineering at Gazi University, Ankara.

He is the founding partner of ANOVA CAD-CAE-TEST, a computer-aided engineering solutions firm. His research interests are computational fluid dynamics and heat transfer applications in defense and aerospace industries.



Ilker Tari received the M.S. degree in nuclear engineering from the University of Michigan, Ann Arbor, in 1991, the Nuclear Engineer and S.M. degrees from the Massachusetts Institute of Technology, Cambridge, in 1994, and the Ph.D. degree in mechanical engineering from Northeastern University, Boston, MA, in 1998.

He is an Assistant Professor of Mechanical Engineering at the Middle East Technical University (METU), Ankara, Turkey. Prior to joining METU, he was with the Mechanical Engineering Department, University of California, Riverside, as a Lecturer. His research interests are computational heat transfer, thermal design, heat exchanger design, microchannel flows, radiative heat transfer, electronics cooling, fuel cells, and solar energy.